J Therm Anal Calorim (2013) 114:131–135
DOI 10.1007/s10973-012-2851-z

Thermal decomposition properties of guanidine nitrate and basic cupric nitrate

Xinliang Mei · Yi Cheng · Yanchun Li · Xuqiang Zhu · Shi Yan · Xiangyu Li

Received: 17 September 2012 / Accepted: 27 November 2012 / Published online: 12 January 2013

Abstract Characterized with a large gas production and low combustion temperature, the guanidine nitrate (GN) gas-generating agents are studied and applied widely. The determination factors of thermal decomposition properties of guanidine nitrate and basic cupric nitrate (GN/BCN) gas-generating agents for airbag application was investigated by the thermogravimetry–differential scanning calorimetry–mass spectrmetry–Fourier transform infrared spectroscopy (TG-DSC-MS-FTIR) and automatic calorimeter. Five different mass ratios were concerned. Our study showed that the onset reaction temperatures of GN/BCN mixtures were lower than that of individual GN and BCN. The thermal decomposition of GN/BCN mixtures could be divided into three stages, including the dissociation and escape of crystal water, solid (GN)-solid (BCN) phase reaction, and liquid (GN)-solid (BCN) phase reaction. When mass ratio of GN/BCN was 62.24/37.73, the largest value of the reaction heat was measured to 3152.7 J g^{-1}, with N_2 and H_2O as the major gases during thermal decomposition.

Keywords Guanidine nitrate · Basic cupric nitrate · Thermal decomposition · Real-time analysis

Introduction

In general, the gas-generating agents are constituted by fuel and oxidizing agents. GN contains rich nitrogen element (49 wt%), and low oxygen demanded [1, 2]. BCN can provide more oxygen, and reduce the combustion heat of gas-generating agent [3, 4]. As containing merits of large gas production and low combustion temperature, the GN/BCN gas-generating agents are being studied and applied widely [3–5]. In 2009, R.S. Damse [6] has studied the mechanism of thermal decomposition of GN, and found out that slow breakage of the relatively strong C–N bond of GN was the major cause for the slow burning behavior of GN. Jimmie C. Oxley et al. [7] have envisioned three possible decomposition routes of GN, and confirmed that nitric acid and NH_3 were dissociated from GN. In 2010, Satoru Yoshino and Atsumi Miyake [8] have researched the thermal decomposition properties of GN and 1,2,4-triazole-3-one (TO) mixtures. They thought that the interaction between TO and nitric acid from the dissociation of GN was proposed for the thermal decomposition of TO/GN mixtures.

For a better understanding of thermal decomposition properties of GN/BCN mixtures, thermogravimetry–differential scanning calorimetry-mass spectrmetry–Fourier transform infrared spectroscopy (TG/DSC-MS-FTIR) and automatic calorimeter were performed.

X. Mei · Y. Cheng (✉) · Y. Li · X. Zhu · S. Yan · X. Li
School of Chemical Engineering, Nanjing University of Science and Technology, Nanjing 210094, People's Republic of China
e-mail: Chengyi20@yahoo.com.cn

X. Mei
e-mail: 412636154@qq.com

Experimental

Materials

The purity of GN (Sanming Coffer Fine Chemical Industrial Co., Ltd) was 98.26 %, and the average particle size was 5.52 μm. The Cu-content and Nitrate-content of BCN (Sanming Coffer Fine Chemical Industrial Co., Ltd) were 52.83 and 24.58 %, respectively. The 50 % accumulative size (D50) was 1.63 μm. Molecular structure of GN was showed as Fig. 1.

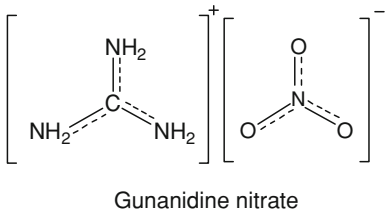

Fig. 1 Molecular structure of GN

Reagents were mixed for sixty minutes using chopsticks on parchment paper carefully [9]. Samples were prepared by mixing a stoichiometric composition and a positive and negative oxygen balance based on Eq. 1. Table 1 shows the mixture compositions.

$$9CH_6N_4O_3(s) + 2[Cu(NO_3)_2{\cdot}3Cu(OH)_2](s) = 9CO_2(g) + 33H_2O(g) + 20N_2(g) + 8Cu(s) \quad (1)$$

Apparatus and method

The heat of reaction was measured using Hunan YouXin YX-ZR Type automatic calorimeter. Benzoic acid was used to calibrate the thermal capacity of automatic calorimeter. Because nickel chrome ignition wire could not ignite GN/BCN mixtures directly, black powder was used to ignite GN/BCN mixtures. 2.5 g of GN/BCN mixtures and 0.3 g of black powder were weighed. Each of the mixtures was tested three times, and took the average.

TG/DSC-MS-FTIR can provide not only the thermal analysis date but also the information of the decomposition gases evolved from the pyrolysis of GN/BCN mixtures. The thermal decomposition process was monitored by MS and FTIR on-line. The apparatus is constituted of three parts: TG/DSC (NETZSCH STA449C) systems, MS (NETESCH-QMS403C) systems, and FTIR (NICOLET6700 FTIR) system. NETESCH-QMS403C conditions: ionizing electron energy of 70 eV, quartz capillary gas connector, pressure injection 1,000 mbar, and capillary temperature 200 °C. NICOLET6700 FTIR conditions: The spectra were integrated 12 times, with a resolution of 4 cm^{-1}, the gas cell and the gas tube between the TG/DSC and the FTIR stayed at 200 °C. All samples were placed in alumina crucibles (80 μL). Samples 1–7 were weighted at 0.30 ± 0.05 mg for the TG/DSC-MS-FTIR tests by heating them at 5 K min^{-1} from 30 to 600 °C. High-purity argon was used as purge gas with a gas flow rate of 20 mL min^{-1}.

Table 1 Composition of mixtures

No.	GN/BCN		Oxygen Balance/g 100 g^{-1}
	Mol ratio	Mass ratio	
1	100.0/0	100.0/0	−26
2	90.90/9.10	71.14/28.86	−10
3	86.64/13.36	62.24/37.76	–5
4	81.82/18.18	53.35/46.65	0
5	75.90/24.10	44.46/55.54	5
6	68.47/31.53	35.57/64.43	10
7	0/100.0	0/100.0	30

Results and discussion

Heat of reaction

In Fig. 2 the heat of reaction results are plotted against the oxygen balance (OB) of GN/BCN mixtures. When the oxygen balance of GN/BCN decreases, the heat of reaction of GN/BCN increases and almost establishes after OB < 0. When oxygen balance of GN/BCN mixtures becomes −5 (mass ratio GN/BCN = 62.64/37.36), then heat of reaction reaches a maximum value (3152.7 J g^{-1}).

Based on Eq. 1, Hess's Law and the relationship between the reaction heat at constant pressure (Q_p) and the reaction heat at constant volume (Q_V), the reaction heat of sample 4 could be calculated.

$$Q_p = \Delta_r H_m^\theta = \sum_i n_i \left(\Delta_f H_m^\theta\right)_i - \sum_p n_p \left(\Delta_f H_m^\theta\right)_p \quad (2)$$

where i is the resultant, p is the reactants, and $\Delta_f H_m^\theta$ is the standard molar enthalpy of formation.

And the reaction heat at constant volume (Q_V)

$$Q_V = Q_p + P_0(V_0 - V) \quad (3)$$

where P_0 is the standard atmospheric pressure, equals 101.325 kPa, V is the volume of all resultants at the standard atmospheric pressure, and V_0 is the volume of oxygen bomb.

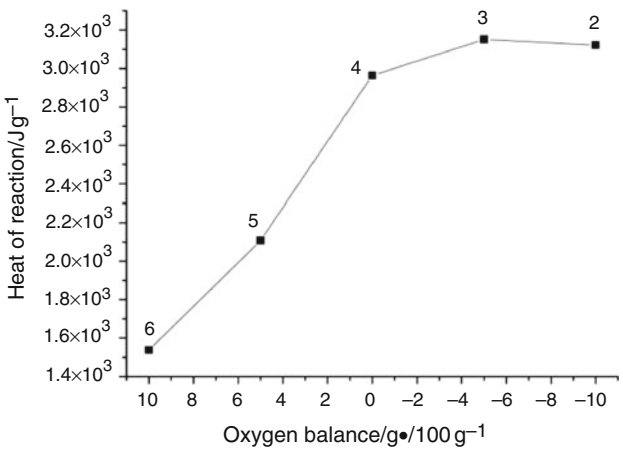

Fig. 2 Heat of reaction versus oxygen balance of GN/BCN mixtures

The volume of oxygen bomb could be ignored and the volume of solid phase in resultants also could be ignored. So

$$Q_V = Q_p - P_0 V_g = Q_p - RNT \quad (4)$$

where V_g is the volume of gas resultants at the standard atmospheric pressure, N is the molar quantity of gas resultants, R is the molar gas constant, equals 8.314 J K^{-1} mol^{-1}, and T is the ambient temperature.

So the calculated value of the reaction heat of GN/BCN is 3006 J g^{-1} (the calculated result is negative, meaning exothermic), and the experimental value is 2964 J g^{-1}, the relative error is only 1.40 %. When oxygen balance is positive (sample 5 and 6), the decomposition of excessive BCN in mixtures need to absorb vast heat, so the heat of reaction is lower than that in zero oxygen balance. When oxygen balance is negative (sample 2 and 3), the combustion of excessive GN in mixtures would emit some heat, so the heat of reaction is slightly higher than that in zero oxygen balance.

Thermal analysis

Figure 3 shows the results of the DSC and TG curves at 5 K min^{-1} heating rates for the pure GN (sample 1), the pure BCN (sample 7) and the mixtures GN/BCN (sample 2–6) with different mass ratios.

Table 2 lists the temperatures at 5 % mass loss ($T_{TG5\ \%}$), onset reactive temperatures (T_{DSC}), the temperature of endothermic peak (T_{p1}), the temperature of first exothermic peak (T_{p2}), and the temperature of second exothermic peak (T_{p3}).

The $T_{TG5\ \%}$ of GN/BCN mixtures is between 160 and 180 °C, the T_{DSC} is between 150 and 170 °C, the T_{p1} is between 170 and 180 °C, the T_{p2} is between 180 and 190 °C, the T_{p3} is near 200 °C. There are no observable difference between each of GN/BCN mixtures about $T_{TG5\ \%}$, T_{DSC}, T_{p1}, T_{p2}, and T_{p3}. But the $T_{TG5\ \%}$ and T_{DSC} of GN/BCN mixtures are lower than those of individual GN and BCN.

Individual GN (sample 1) has three peaks. The first endothermic peak at 213 °C in the DSC curve corresponds to the phase change from solid to liquid. After this phase change, the main decomposition of GN begins at about 278 °C and completed at 320 °C (72.8 % mass loss). Ref. [10] considered that the endothermic decomposition is caused by the decomposition of NH_4NO_3 or the dissociation and escape of $HNO_3 + NH_3$. Meanwhile, a kind of polymer production called Melon is prepared from the intermediate (H_2N–C ≡ N) by multi-step polymerization. And the third endothermic peak at higher temperature is the decomposition of Melon [6, 7, 10].

DSC/TG curves of the pure BCN (sample 7) show that the decomposition reaction starts at about 219 °C and ends with a 34 % loss in mass. The mass ratio of CuO in BCN is about 66.25 %, and the mass ratio of Cu_2O in BCN is about 59.58 %. It indicated that most of the solid residue of thermal decomposition of BCN is CuO.

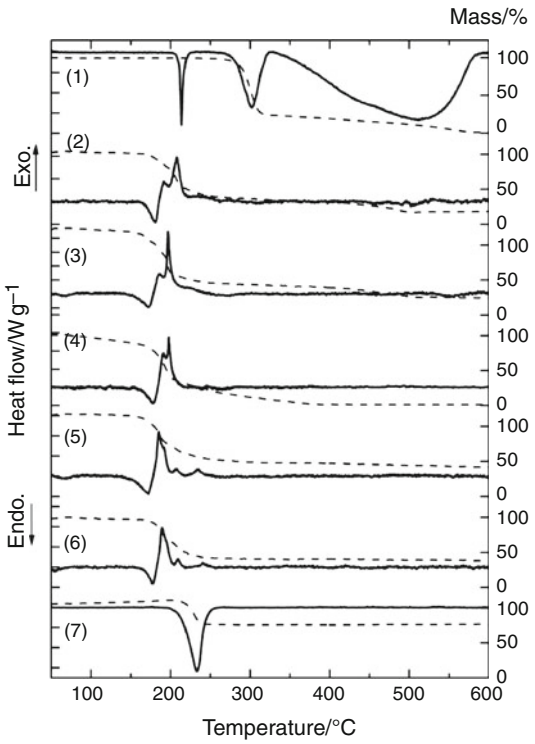

Fig. 3 TG-DSC *curves* of GN/BCN mixtures

Table 2 Results of thermal analysis of GN/BCN mixtures

No.	$T_{TG5\ \%}$/°C	T_{DSC}/°C	T_{p1}/°C	T_{p2}/°C	T_{p3}/°C
1	279	278	–	213*	302**
2	176	167	179	187	205
3	162	152	172	184	196
4	176	165	178	190	199
5	164	154	171	185	205
6	177	166	177	189	208
7	219	204	233***	–	–

* the melting peak of GN, ** the decomposition peak of GN, *** the decomposition peak of BCN

There are three main peaks in the decomposition process of GN/BCN mixtures. So the thermal decomposition of GN/BCN mixtures could be divided into three stages. The first endothermic peak between 170 and 180 °C is thought to be the dissociation and the escaping of crystal water (DSC-MS curve could explain it). The second peak is an exothermic peak at about 185 °C. The ratio between the value of the second peak and the value of the third peak becomes larger with an increase of BCN in GN/BCN

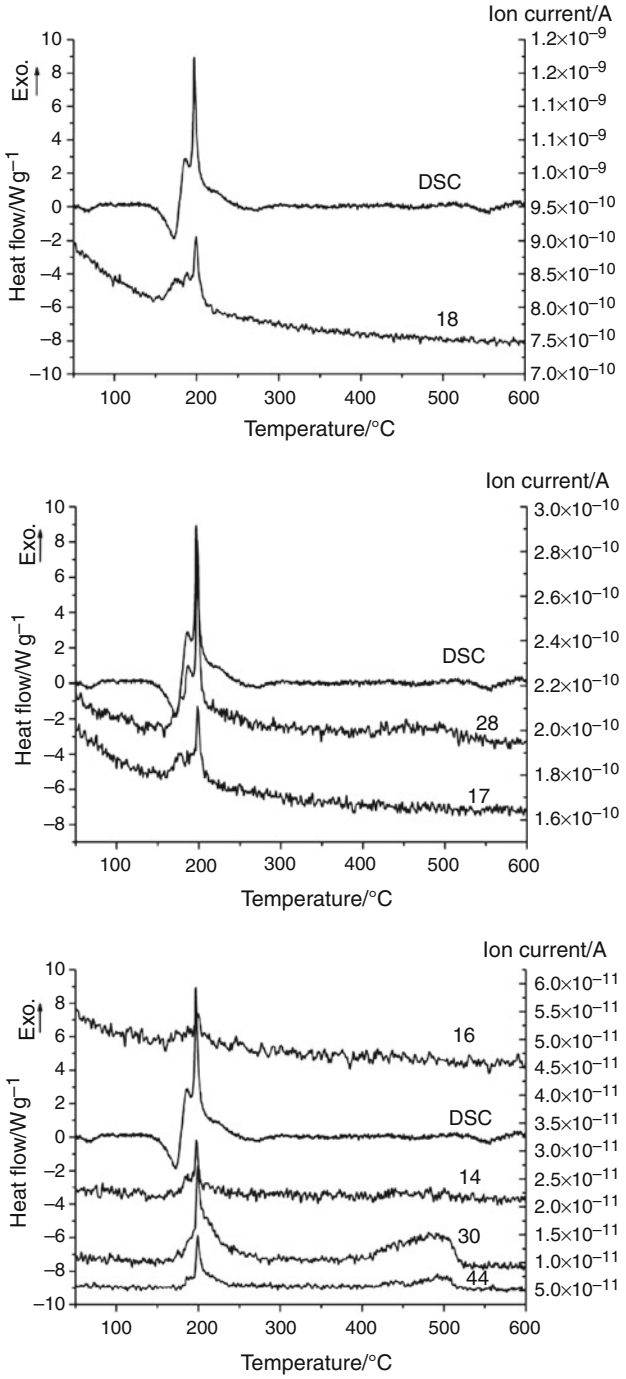

Fig. 4 DSC-MS (m/z = 14, 16, 17, 18, 28, 30, 40) curve of sample 3

mixtures. And the peak temperature is significantly lower than the onset melting temperature (198 °C) of pure GN and the onset decomposition temperature (204 °C) of BCN. Hence, the reactive of GN/BCN mixtures is considered to be a solid (GN)-solid (BCN) phase reaction. The third peak is still an exothermic peak at about 200 °C. The value of third peak becomes lower with an increase of BCN in GN/BCN mixtures. The exothermic peak near 200 °C which is slightly higher than the onset melting temperature (198 °C)

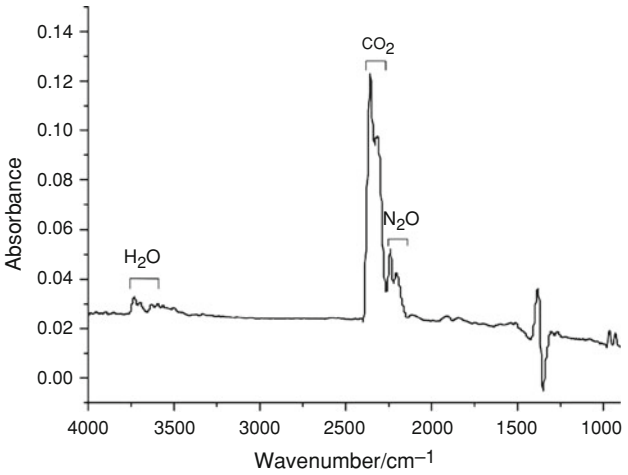

Fig. 5 The FTIR spectra of gas products of sample 3 at 200 °C

of GN and lower than the onset decomposition temperature (204 °C) of BCN is thought to be a liquid (GN)-solid (BCN) phase reaction, which increases the contact area of GN and BCN and making the reaction more intense. When the oxygen balance is positive, the weak exothermic peak is thought to be a combined effect of the exothermic reaction of GN/BCN and the endothermic decomposition of excess BCN.

Gas products analysis

Evolved gas analyses are performed using TG/DSC-MS-FTIR. Figure 4 represents the DSC-MS of the gas products of sample 3. It can be found that the m/z = 14(N), 16(O or NH_2), 17(OH or NH_3), 18(H_2O), 28(CO or N_2), 30(NO), and 44(CO_2 or N_2O) are detected. Figure 5 shows the FTIR spectra of gas products of sample 3 at 200 °C. The IR spectral peaks are assigned to νN_2O: ~2,238 cm^{-1}, νCO_2: ~2,368 cm^{-1}, δH_2O: 3,500–3,800 cm^{-1} [11]. Comparing Fig. 4 with 5, it is certain that there are H_2O, N_2, N_2O, and CO_2, and almost no NO (1,965–1,762 cm^{-1}) and CO (2,176 cm^{-1}). Figure 4 shows only m/z = 17 and 18 have corresponding weak peak compared with endothermic peak of DSC at about 180 °C, so the initial endothermic reaction of GN/BCN mixtures in the range of 150–180 °C is thought to be dissociation and escape of chemical water.

Conclusions

Based on the investigation of the thermal decomposition properties of GN/BCN mixtures, the following conclusions were drawn.

1 The heat of reaction for OB (GN/BCN) = −5 is larger than those of other mixing ratios.

2 The initial reactive temperatures of GN/BCN mixtures are significantly lower than the decomposition temperature of BCN and the melting temperature of GN.
3 The reaction of GN/BCN mixtures could be divided into three stages. And the main stages include the dissociation and escape of crystal water, solid (GN)-solid (BCN) phase reaction and liquid (GN)-solid (BCN) phase reaction.
4 The gases evolved from GN/BCN mixtures are determined to be H_2O, N_2, and N_2O. H_2O and N_2 are the major gases for the thermal decomposition of GN/BCN mixtures.

References

1. Mendenhall IV, Smith RG. Microgas-generating agent [P]. CN Patent 03812220.0. 2003.
2. Ulas A, Risha GA, Kuo KK. Ballistic properties and burning behaviour of an ammonium perchlorate/guanidine nitrate/sodium nitrate airbag solid propellant. Fuel. 2006;85:1979–86.
3. Jianzhou W. Gas-generating agent composition [P]. CN Patent 200410086968.7. 2003.
4. Jianzhou W. Gas-generating agent composition [P]. CN Patent 03801083.6. 2003.
5. Seo YD, Chung SH, Yoh JJ. Automotive airbag inflator analysis using the measured properties of modern propellants. Fuel. 2011; 90:1395–401.
6. Damse RS. Studies on the decomposition chemistry of triamino guanidineazide and guanidine nitrate. J Hazard Mater. 2009;172: 1383–7.
7. Oxley JC, Smith JL, Naik S, Moran J. Decompositions of urea and guanidine nitrate. J Energ Mater. 2009;27:17–39.
8. Yoshino S, Miyake A. Thermal decomposition properties of 1,2,4-triazole-3-one and guanidine nitrate mixtures. J Therm Anal Calorim. 2010;102:513–6.
9. Akiyoshi M, Nakamura H, Hara Y. The thermal behavior of the zinc complexes as a non-azide gas generant for safer driving—Zn complexes of the carbohydrazide and semicarbazide. Propellants, Explos Pyrotech. 2000;25:41–6.
10. Liu Z. Thermal analyses for energetic materials. Beijing: National Defense Industry Press; 2008. p. 184–6.
11. Li Y, Cheng Y. Investigation on the thermal stability of nitroguanidine by TG/DSC-MS-FTIR and multivariate non-linear regression. J Therm Anal Calorim. 2010;100:949–53.